

Comparison of Cardiac Diffusion Tensor and Generalized Q-Sampling MRI

Eric P. Aliotta^{1,2}, Marmar Vaseghi³, Kalyanam Shivkumar³, and Daniel B. Ennis^{1,2}

¹Biomedical Physics IDP, University of California, Los Angeles, CA, United States, ²Department of Radiological Sciences, University of California, Los Angeles, CA, United States, ³Cardiac Arrhythmia Center & EP Programs, University of California, Los Angeles, CA, United States

INTRODUCTION – Diffusion tensor MRI (DT-MRI) accurately characterizes the myofiber organization of cardiac tissue with the primary eigenvector (ε_1), but has several limitations that confound evaluation of the sheet-like myolaminar structure including limited angular resolution, *de facto* orthogonality of the principal directions of diffusion, and a lack of clear, empirical distinction between the secondary (ε_2) and tertiary (ε_3), directions of diffusion. More recently generalized Q-sampling MRI (GQ-MRI) has emerged as a technique that overcomes these DT-MRI limitations. GQ-MRI encodes diffusion across a dense lattice of q-space vectors and requires no assumptions about the directionality of diffusion. The ε_2 and ε_3 directions characterize the orientation of myocardial laminae (sheets) and are critical to our understanding of ventricular mechanics, electrophysiology of arrhythmias and electrical wave propagation. However, these directions as provided by DT-MRI are sometimes ambiguously ordered and of limited angular certainty [1]. The objective of this study was to compare the microstructural information provided by DT-MRI and GQ-MRI in *ex vivo* infarcted porcine hearts. We hypothesized that GQ-MRI will estimate the same ε_1 directions as DT-MRI, but will provide different measures of the ε_2 and ε_3 directions.

METHODS – Porcine hearts (N=4) were imaged *ex vivo* with a 3.0T scanner (Siemens Trio, Erlangen, Germany) using 515 combinations of b-values and directions and a stimulated echo diffusion protocol ($b_{\max}=4000$ s/mm², one $b=0$ acquisition, 2.5 x 2.5 x 5 mm resolution, TE/TR=77/6800ms, 5 averages, scan time=9 hrs 45 minutes). Spin density functions (SDFs) were reconstructed using the GQ-MRI framework in DSI Studio (<http://dsi-studio.labsolver.org/>) and used to derive three principle diffusion directions. ε_1 was defined by the orientation of the largest SDF peak. ε_2 and ε_3 were determined by local maxima on the surface of the SDF. ε_2 and ε_3 are by definition orthogonal to ε_1 , but there is no constraint on the angle between them. DT-MRI were reconstructed in Matlab (Mathworks, Natick, MA) from a subset of the GQ-MRI data acquired with a constant b-value of 2000 s/mm² (46 directions) and one b-value=0 acquisition. The median±95% confidence interval ($\Delta\varepsilon_i$, $\varepsilon_i=[\varepsilon_1, \varepsilon_2, \varepsilon_3]$) and maximum likelihood (σ_i) angle between each GQ-MRI and DT-MRI principal direction were calculated throughout the myocardium. The angle between GQ-MRI ε_2 and ε_3 directions (ξ) was also evaluated for orthogonality. Data were pooled from all four hearts before the statistical analysis was performed.

RESULTS – Qualitative maps of ε_1 are shown in Fig. 1. The ε_1 directions of diffusion reported by GQ-MRI and DT-MRI were in good agreement ($\Delta\varepsilon_1=7.1^\circ$ [1.3°, 47.6°] $\sigma_1=5^\circ$). Differences in ε_1 were larger in voxels where more than one fiber population was resolved ($\Delta\varepsilon_1=18.3^\circ$ [2.2°, 77.8°], $\sigma_1=9^\circ$) compared to single-fiber voxels ($\Delta\varepsilon_1=6.2^\circ$ [1.2°, 26.5°], $\sigma_1=5^\circ$). $\Delta\varepsilon_1$ increased near the base of the heart, where multiple fiber populations were resolved by GQ-MRI in a larger number of voxels. The ε_2 and ε_3 GQ-MRI and DT-MRI directions did not agree as closely ($\Delta\varepsilon_2=24.8^\circ$ [3.3°, 82.0°], $\sigma_2=11^\circ$, $\Delta\varepsilon_3=34.2^\circ$ [3.6°, 84.3°], $\sigma_3=20^\circ$). These differences were not correlated with the number of fibers resolved. Distributions of $\Delta\varepsilon_1$, $\Delta\varepsilon_2$ and $\Delta\varepsilon_3$ are shown in Fig. 2. The ε_2 and ε_3 GQ-MRI directions were not orthogonal, the angle between them tended to be less than 90° ($\xi=78.1^\circ$ [4.8°, 89.9°]).

DISCUSSION – GQ-MRI provides the probability of diffusion as a function of directionality. However, when q-space imaging is reported, this data is frequently reduced to the primary orientations of fiber populations. In this study, we also evaluated the shape of the SDF to characterize the anisotropy of diffusion in myocardium. These measurements contain information about the organization of myocardial sheet structure as well as provide a framework for comparison with the more extensively studied tensor representation. While $\Delta\varepsilon_1$ was relatively low and consistent with previous reports of ε_1 angle differences between DT-MRI and histology [1,2], it might be expected that $\Delta\varepsilon_1$ would be even smaller for reconstructions of the same data. This bias may infer that GQ-MRI estimates are more accurate given the model-free reconstruction. The finding that $\Delta\varepsilon_1$ was correlated with the number of resolved fibers may infer that GQ-MRI better represents myofiber orientation than DT-MRI in the presence of multiple fiber populations. $\Delta\varepsilon_2$ and $\Delta\varepsilon_3$ were larger, which indicates significant discrepancy between the ε_2 and ε_3 principal directions of diffusion reported by DT-MRI and GQ-MRI. Again, given the model-free representation of the SDF the GQ-MRI ε_i are likely to better represent the myolaminar organization of the heart. Notably, ξ significantly deviated from 90°, which again highlights the importance of model-free estimates of the principal directions of diffusion.

CONCLUSION – The agreement between GQ-MRI and DT-MRI in primary diffusion direction indicates that both frameworks similarly describe myofiber orientation. The significant disagreement in the ε_2 and ε_3 directions indicates that DT-MRI may not accurately characterize the organization of myolaminar sheets.

REFERENCES — [1] Kung GL *et al. JMRI* 2011. **34**(5): p. 1080-91. [2] Scollan, DF *et al. AJP* 1998. **275**(6): H2308-H2318

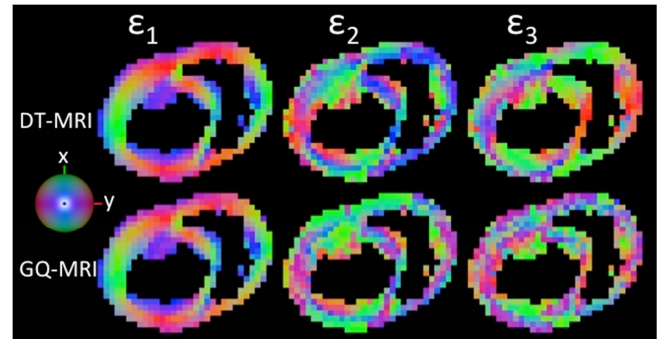


Figure 1: XYZ-RGB Map of ε_1 , ε_2 , ε_3 from DT-MRI and GQ-MRI.

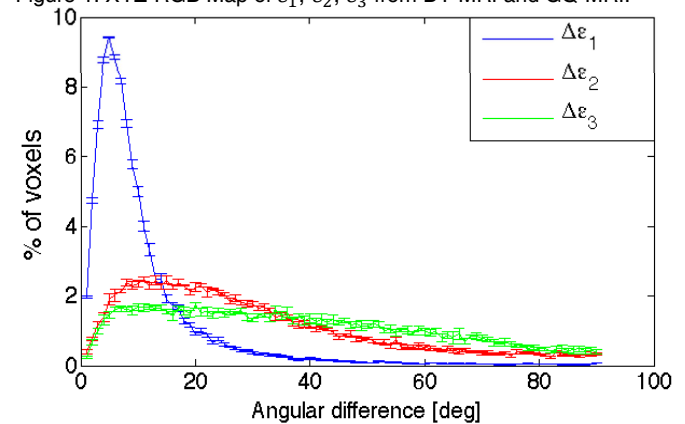


Figure 2: Percentage of voxels versus $\Delta\varepsilon_1$, $\Delta\varepsilon_2$, $\Delta\varepsilon_3$.